



Aerosols in the lung: multi-domain transport and coupling

Jessica M. Oakes, Shawn C. Shadden, Céline Grandmont, Irene Vignon-Clementel

► To cite this version:

Jessica M. Oakes, Shawn C. Shadden, Céline Grandmont, Irene Vignon-Clementel. Aerosols in the lung: multi-domain transport and coupling. 4th International Conference on Computational and Mathematical Biomedical Engineering - CMBE2015, Jun 2015, Cachan, France. hal-01244582

HAL Id: hal-01244582

<https://hal.inria.fr/hal-01244582>

Submitted on 16 Dec 2015

HAL is a multi-disciplinary open access archive for the deposit and dissemination of scientific research documents, whether they are published or not. The documents may come from teaching and research institutions in France or abroad, or from public or private research centers.

L'archive ouverte pluridisciplinaire **HAL**, est destinée au dépôt et à la diffusion de documents scientifiques de niveau recherche, publiés ou non, émanant des établissements d'enseignement et de recherche français ou étrangers, des laboratoires publics ou privés.

AEROSOLS IN THE LUNG: MULTI-DOMAIN TRANSPORT AND COUPLING

Jessica M. Oakes^{1,2,3}, Shawn C. Shadden¹, Céline Grandmont^{2,3,*}, and Irene E. Vignon-Clementel^{2,3,*}

¹University of California Berkeley, Department of Mechanical Engineering, Berkeley, CA, USA

²INRIA Paris-Rocquencourt, FRANCE

³Laboratoire Jacques-Louis Lions, Sorbonne Université UPMC Univ Paris 6, FRANCE

*co-senior authors, Email Contacts: J. OAKES: jessica.m.oakes@gmail.com, C. GRANDMONT: celine.grandmont@inria.fr, S. SHADDEN: shadden@berkeley.edu, I.

VIGNON-CLEMENTEL: irene.vignon-clementel@inria.fr

SUMMARY

In this paper, we present a framework that couples three-dimensional (3D) to one-dimensional (1D) transport models to predict particle deposition in the respiratory airways throughout respiration. During respiration, the time dependent flow rate and particle concentration can be passed between the domains (inspiration: 3D to 1D, expiration: 1D to 3D). This framework enables us to predict particle transport and deposition in the whole lung and throughout both inspiration and expiration.

Key words: *computational fluid dynamics, particles, respiratory tract, inspiration and expiration*

1 INTRODUCTION

Recent advances in computational resources have enabled sophisticated airflow and particle transport simulations in the pulmonary airways, however it is currently unfeasible to solve for airflow and transport for all length scales of the lung. Furthermore, while there has been significant focus on predicting particle transport during inspiration [8, 4, 3], there is limited knowledge on particle fate during expiration.

Our group recently developed a computational framework to simulate airflow and particle transport in the conducting airways of the lung [9]. We showed favorable agreement between the simulation predictions and *in vivo* experimental data [8] for lobar deposition fractions in healthy rat lungs. However, we assumed that the number of deposited particles is proportional to the number of delivered particles and is the same for each lobe. However, due to the lobe-specific airway branching structure [6], this assumption may not be valid. Furthermore, this assumption is likely inaccurate in emphysema, a chronic obstructive pulmonary disease [8].

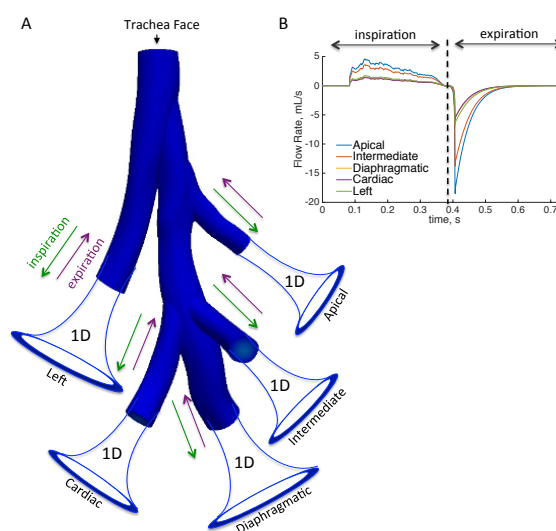


Figure 1: 3D-1D particle coupling illustration between the 3D image-based airways and 1D trumpet models (panel A). Panel B shows the flow rate of each lobe determined from the 3D flow simulation [9]. This lobe-specific flow rate, Q_0 , was employed to solve the 1D flow model.

2 METHODOLOGY

3D Flow and Transport Models: Airflow and particle transport in the 3D domain has been described previously [9, 8] and thus only briefly discussed here. Airflow was found by solving the incompressible Navier-Stokes equations by employing finite element methods. A custom linear solver was employed which incorporated a resistance-based pre-conditioner with a combination of GMRES and conjugate gradient methods [1]. A mechanical ventilation pressure waveform was prescribed at the trachea face and resistance and compliance lumped parameter models were implemented at each of the distal faces. To ensure numerical stability a convection stabilization scheme [2] was employed at the boundary faces. Flow waveforms at each distal face (Figure 1B) was determined from the 3D flow simulation and employed in the 1D model. In the 3D domain the particle trajectory was determined by solving a reduced form of the Maxey-Riley equation by Lagrangian methods, thus each individual particle is convected by the hydrodynamic forces imposed by the flow field obtained from the 3D Navier Stokes solution. Convergence of the solution was determined for both the mesh size and number of particles simulated.

1D Flow and Transport Models: A single path convection-diffusion model [11] was employed to determine transport in the airways peripheral to the 3D geometry and is given as

$$\frac{\partial[A_E(x,t)c(x,t)]}{\partial t} = \frac{\partial}{\partial x} \left[D(x,t)A(x) \frac{\partial c(x,t)}{\partial x} \right] - \frac{\partial[Q(x,t)c(x,t)]}{\partial x} - L(x,t)c(x,t). \quad (1)$$

where $c(x,t)$ is the concentration ($\frac{\text{mass}}{\text{volume}}$), $A(x)$ is the bronchial cross-sectional area, $A_E(x,t)$ includes $A(x)$ and the additional area due to the alveoli, $Q(x,t)$ is the flow rate in the conduits, $D(x,t)$ is the effective diffusion due to mixing in the airways, and $L(x,t)$ is the deposition loss term. With this model, all airways within a given generation are lumped together. The airways in the alveolar region of the lung expand and contract throughout respiration. The loss term, $L(x,t)$, models deposition due to gravitational, inertial and diffusive forces based on empirical models [11]. The 1D continuity equation is solved for $Q(x,t)$, $\frac{\partial Q}{\partial x} = \frac{\partial A_E}{\partial t}$ with $Q(0,t) = Q_0$ and $Q(x,0) = 0$. Q_0 is the flow rate at each distal airway found from the 3D Navier-Stokes solver (Figure 1B). As $\int_0^L A_E = V_{T_i}$, where V_{T_i} is the inspired volume of each lobe, the flow rate approaches 0 at the last airway generation. Equation 1 is solved with an semi-implicit finite volume scheme [5]. The initial condition for inspiration was set to $c(x,0) = 0$ and the boundary conditions were set to $c(0,t) = c_0$ and $\frac{\partial c}{\partial x} \Big|_{x=L} = 0$, where c_0 is the concentration at the 3D-1D coupled surface. For expiration, the boundary conditions are taken as: $\frac{\partial c}{\partial x} \Big|_{x=0} = 0$, and $\frac{\partial c}{\partial x} \Big|_{x=L} = 0$. A mass convergence study of the numerical scheme was performed. Lobe specific airway dimensions were employed [12] and were scaled to represent a lung at functional residual capacity (FRC).

3D-1D Particle Coupling: With this framework particles can be passed between the two domains throughout respiration (inspiration: 3D to 1D, expiration: 1D to 3D, Figure 1). Particles then either exit the distal airways of the 3D domain or deposit on the airway walls. If the particles exit the 3D model they will be passed to the 1D model. For the 3D and 1D domains a Lagrangian and Eulerian approach is taken, respectfully. Thus, the description of particles must be converted at the 3D-1D interface. For inspiration the particle concentration is calculated by dividing the mass of particles exiting the model by the volume of air the particles were suspended in. Particles were released back into the 3D model at each 3D-1D interface throughout expiration. The number of particles to be released during expiration was prescribed such that there was convergence of the solution.

Comparison of Model Predictions to Experimental Data: The 3D-1D simulated results were compared to experimental data [8, 10] by

$$VP_{dep_i} = \frac{P_{dep_i}}{\alpha_i} \quad (2)$$

where P_{dep_i} is the number of particles deposited in each lobe normalized by the total lung deposition and α_i is the volume of each lobe divided by the total volume of the lung. Similarly, for the 3D simulation, VP_{del_i} was calculated, where del is the number of particles delivered to the lobe.

3 RESULTS AND CONCLUSIONS

Volume normalized deposition results are given in Figure 2. Values of 1 indicate that the particle deposition (3D-1D or experimental data) or delivery (3D only) is directly proportional to the volume fraction. Good agreement was found between model predictions and the experimental data of Oakes et al. [7], with the exception of the cardiac lobe. However all predictions matched well with the experimental data of Raabe et al. [10]. Deposition was found to be dependent on lobar specific geometric parameters (e.g. path length to start of acinus).

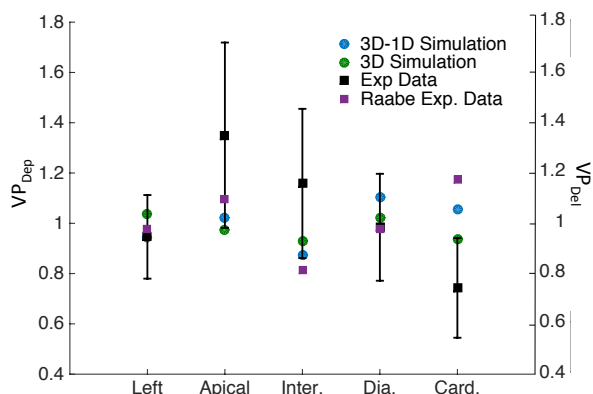


Figure 2: Preliminary comparison of simulations results with experimental data of Oakes et al. [9] and Raabe et al. [10]. Definitions of VP_{dep_i} and VP_{del_i} are given in the Methodology Section. The 3D simulation results are for only the 3D model and the 3D-1D Simulation results is for the coupled model. Results are for particles with MMAD of $1.2 \mu m$.

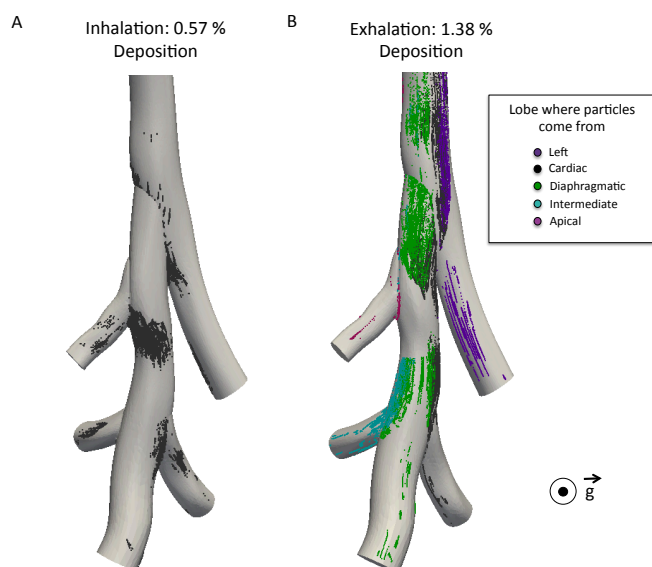


Figure 3: Preliminary results showing particle deposition sites during inspiration (Panel A) and expiration (Panel B). Particle deposition location based on lobe particle was originating from is shown for the exhalation simulation. Deposition percentages are calculated by the number of particles depositing normalized by the number of particles entering the 3D model.

out both inspiration and expiration, facilitating physiologically realistic deposition predictions. This framework may be applied in future studies to determine lung burden in diseased lungs (e.g. patients with chronic obstructive pulmonary disorder (COPD) or asthma). Future work should also include comparing the 1D single-path model to a 1D multiple-path model. A 1D multiple-path model will

Figure 3 shows the predicted deposition during inhalation (panel A) and exhalation (panel B). The percentage of deposited particles was calculated as the number of particles depositing normalized by the total number of particles entering the 3D model. More particles deposited during the exhalation phase of respiration than during the inhalation phase (Figure 3). This enhanced deposition is caused by the slow flow rate during the last 0.1 seconds of exhalation. During this time, the particles suspended in the airway have time to sediment and deposit on the airway walls.

In this work, we demonstrated the ability to couple a 3D model, where flow and particle transport are complex, to a 1D single path model. With this new framework, we have the ability to perform whole lung simulations. Additionally, we can now predict regional deposition through-

enable direct comparison between 1D models and 3D simulations.

Acknowledgments: This work was supported by an University of California Presidential Postdoctoral Fellowship (J. Oakes) and an INRIA Associated Postdoctoral Grant (J. Oakes).

REFERENCES

- [1] M. Esmaily Moghadam, Y. Basikevs, and A. L. Marsden. A new preconditioning technique for implicitly coupled multidomain simulations with applications to hemodynamics. *Computational Mechanics*, 52:1141–1152, 2013.
- [2] M. Esmaily Moghadam, Y. Bazilevs, T.-Y. Hsia, I. E. Vignon-Clementel, and A. L. Marsden. A comparison of outlet boundary treatments for prevention of backflow divergence with relevance to blood flow simulations. *Computational Mechanics*, 48(3):277–291, April 2011.
- [3] P. W. Longest and S. Vinchurkar. Effects of mesh style and grid convergence on particle deposition in bifurcating airway models with comparisons to experimental data. *Medical Engineering and Physics*, 29(3):350–66, April 2007.
- [4] B. Ma and K. R. Lutchen. CFD simulation of aerosol deposition in an anatomically based human large-medium airway model. *Annals of Biomedical Engineering*, 37(2):271–85, February 2009.
- [5] Sébastien Martin and Bertrand Maury. Modeling of the oxygen transfer in the respiratory process. *ESAIM: Mathematical Modelling and Numerical Analysis*, 47(4):935–960, June 2013.
- [6] J M Oakes, M Scadeng, E C Breen, A L Marsden, and C Darquenne. Rat airway morphometry measured from in-situ MRI-based geometric models. *Journal of Applied Physiology*, 112:1921–1931, March 2012.
- [7] Jessica M. Oakes, Ellen Breen, Miriam Scadeng, Ghislain S. Tchantchou, and Chantal Darquenne. MRI-based measurements of aerosol deposition in the lung of healthy and elastase-treated rats. *Journal of Applied Physiology*, 116:1561–1568, 2014.
- [8] Jessica M. Oakes, Alison L. Marsden, Céline Grandmont, Chantal Darquenne, and Irene E. Vignon-Clementel. Distribution of aerosolized particles in healthy and emphysematous rat lungs: Comparison between experimental and numerical studies. *Journal of Biomechanics*, 48(6):1147–1157, 2015.
- [9] Jessica M Oakes, Alison L Marsden, Celine Grandmont, Shawn C Shadden, Chantal Darquenne, and Irene E Vignon-Clementel. Airflow and particle deposition simulations in health and emphysema: from in vivo to in silico animal experiments. *Annals of Biomedical Engineering*, 42(4):899–914, April 2014.
- [10] Otto G. Raabe, Mohamed A. Al-Bayati, Stephen V. Teague, and Amiram Rasolt. Regional deposition of inhaled monodisperse Coarse and fine aerosol particles in small laboratory animals. *Annals Occupational Hygiene*, 32(6):53–63, 1988.
- [11] D B Taulbee and C P Yu. A theory of aerosol deposition in the human respiratory tract. *Journal of applied physiology*, 38(1):77–85, January 1975.
- [12] H C Yeh, G M Schum, and M T Duggan. Anatomic models of the tracheobronchial and pulmonary regions of the rat. *The Anatomical Record*, 195(3):483–92, November 1979.